Ganguly et al., https://doi.org/10.1083/jcb.201604028

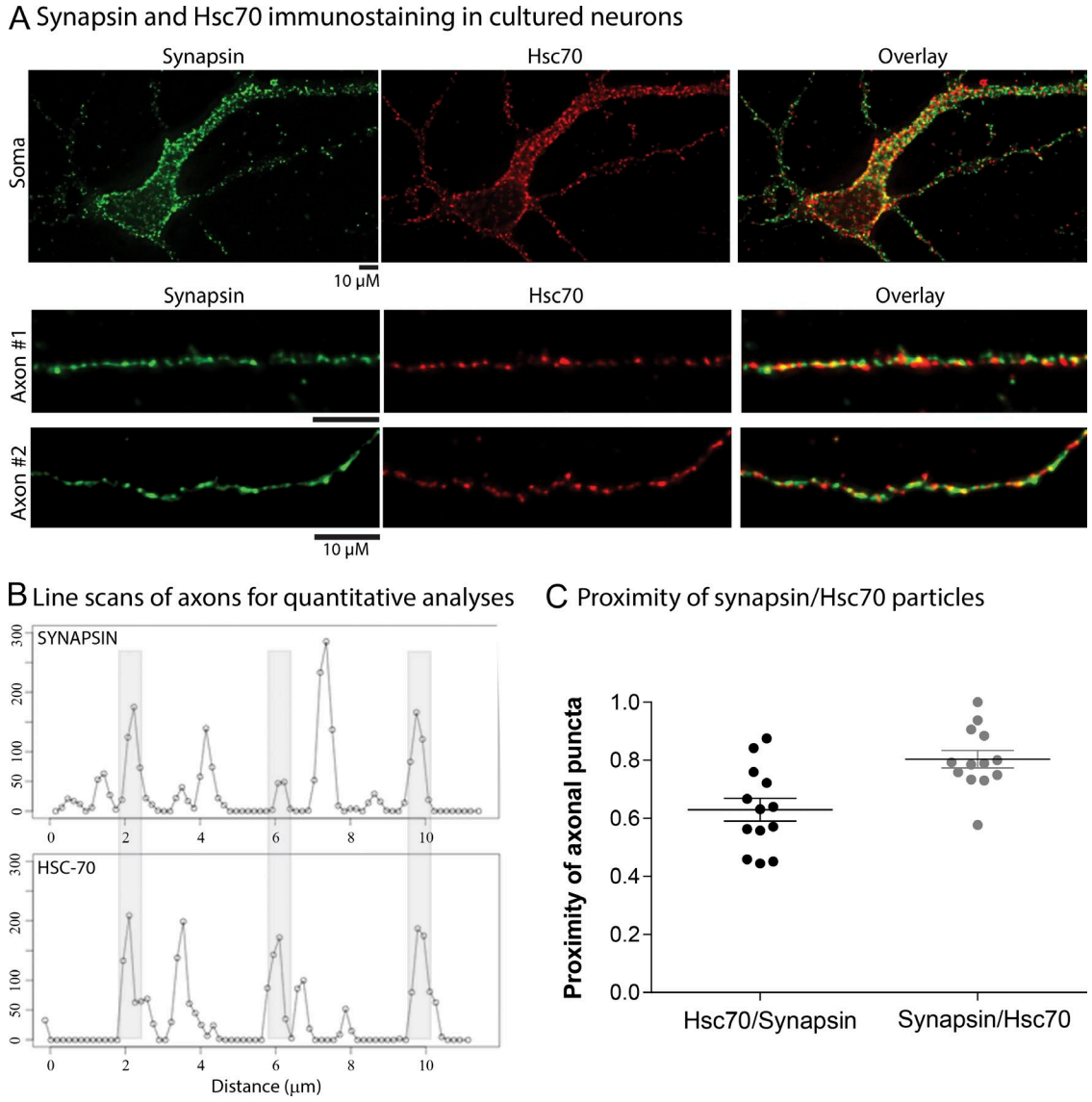

Figure S1. **Endogenous synapsin and Hsc70 distribution in cultured hippocampal neurons.** (A) Representative images show endogenous immunostaining of synapsin (green) and Hsc70 (red) in the soma (top) and axon segments (bottom) from cultured hippocampal neurons (yellow overlay). (B) To quantify the proximity of endogenous synapsin and Hsc70 particles in axons, derivative peak analysis of axon ROIs was performed (see the Colocalization analysis of widefield images… section of Materials and methods for details). Representative line scans from an axon ROI show the distribution of endogenous synapsin and Hsc70 along the length of the axon. Light gray bars are instances where synapsin and Hsc70 puncta occurred in close proximity. (C) Cumulative analysis of axon ROIs (n = 13 axons) reveals close proximity between synapsin and Hsc70 particles. The y axis represents a proximity index where a value of 1.0 represents complete overlap of particles.

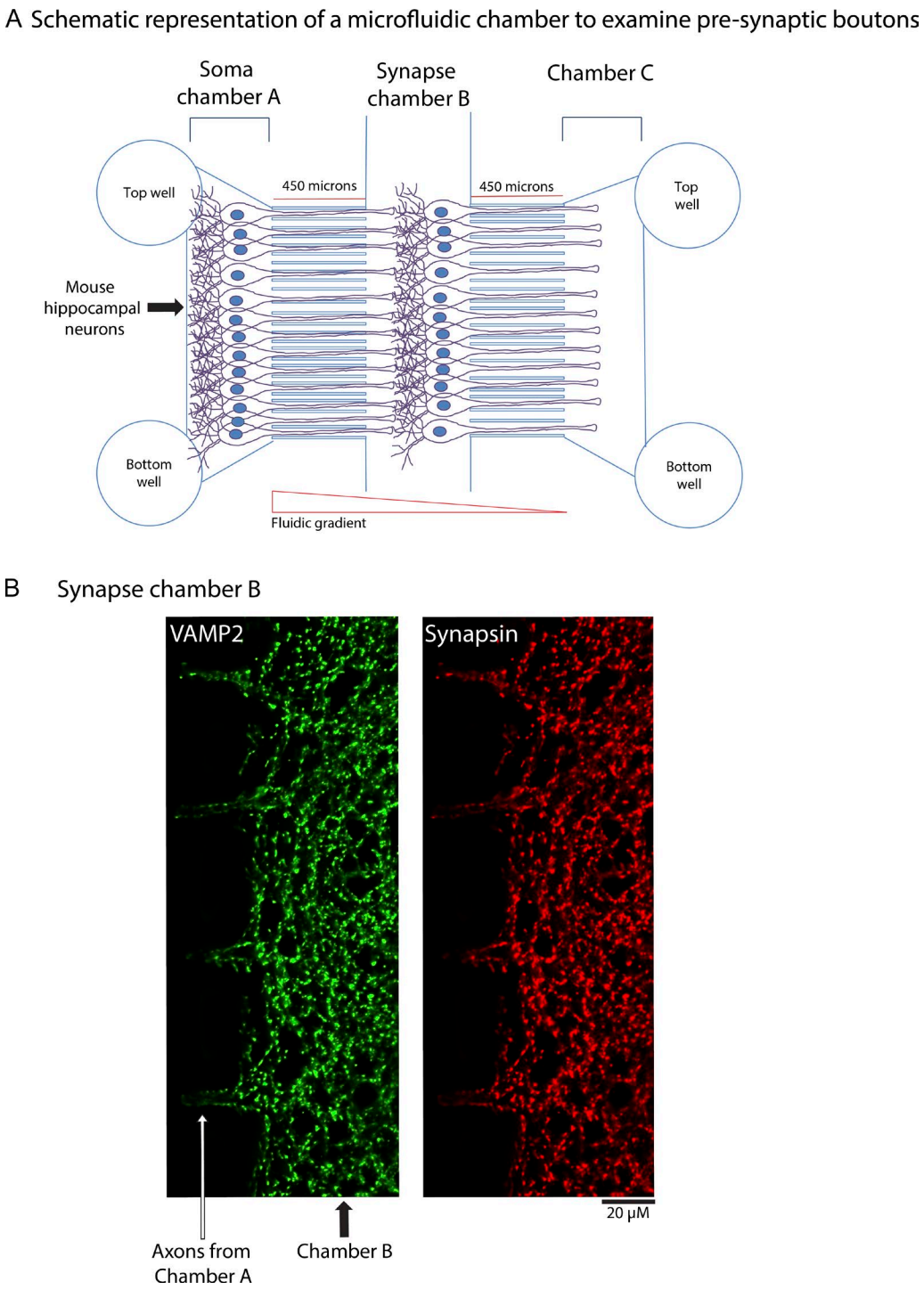

Figure S2. **Microfluidic device to examine presynaptic boutons.** (A) Strategy used to examine presynaptic boutons. Hippocampal neurons were plated in chambers A and B, and a descending fluidic gradient was maintained from A to C, ensuring that axons from neurons in chamber A entered chamber B and synapsed onto the neurons in chamber B, thus forming functional presynaptic boutons. The effect of drug treatments on axonal transport and synaptic delivery was studied by application of drug to chamber A and examining presynaptic boutons in chamber B. (B) Representative images from chamber B (black arrow) of one such device described in A. The device is fixed and immunostained at DIV 12 for a synaptic bouton marker (VAMP2; left) and synapsin (right). Axons are seen in the microgrooves connecting chambers A and B (white arrow).

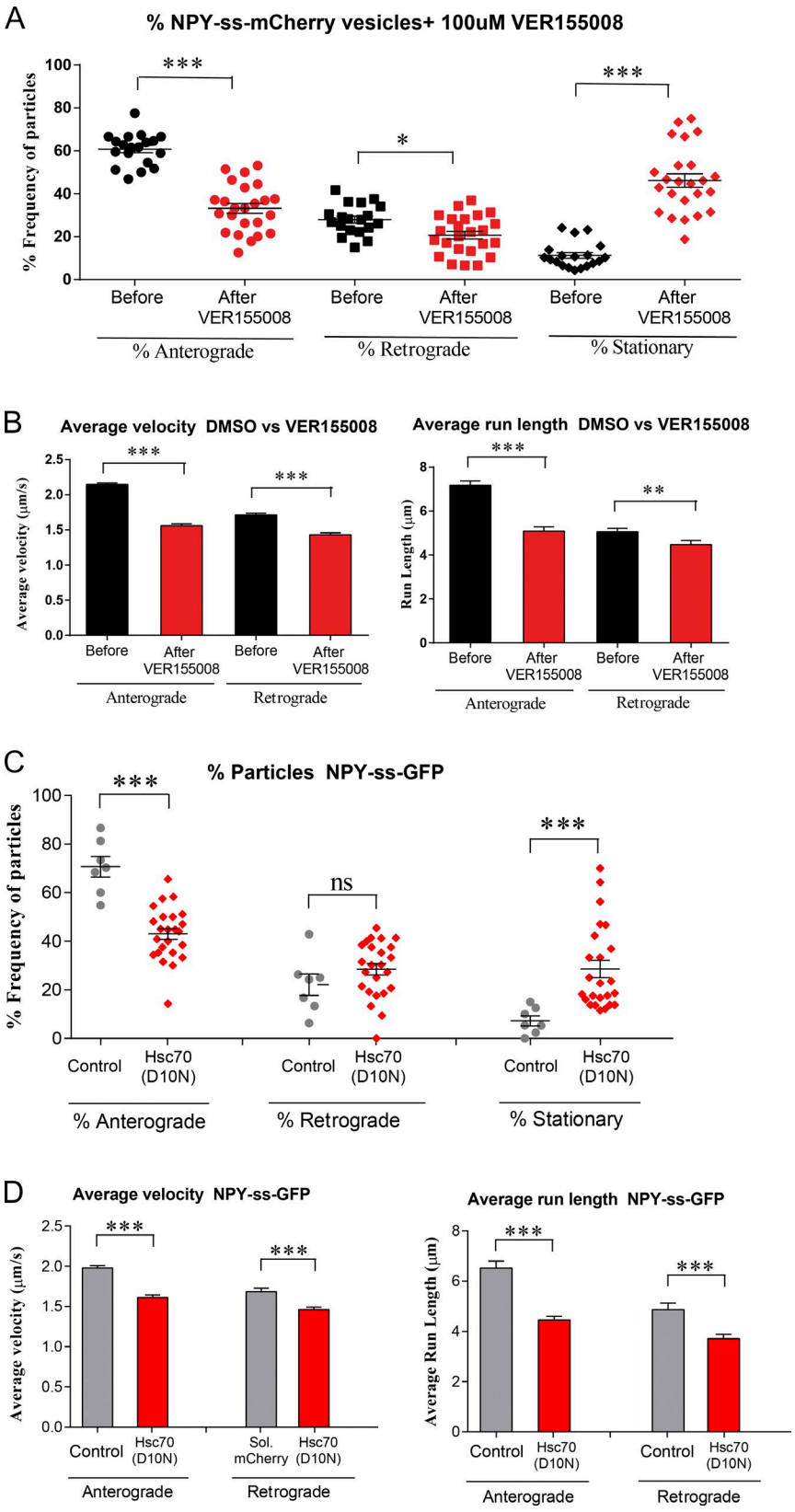

Figure S3. **Effects of Hsc70 ATPase inhibition on fast vesicle transport.** (A–D) Cultured hippocampal neurons were transfected with NPY-ss–mCherry (pan-vesicle marker), and axonal transport was analyzed after Hsc70 inhibition. (A and B) Quantitative NPY-ss transport data from experiments where axonal transport was evaluated before and after adding the Hsc70 ATPase inhibitor VER155008. (C and D) Quantitative NPY-ss transport data from experiments where neurons were either transfected with a soluble marker (soluble mCherry) or a dominant-negative Hsc70 (Hsc70-D10N:mCherry). Note attenuation of both anterograde and retrograde transport in these experiments. All values represent means ± SEM. P-values were obtained via unpaired *t* test. Error bars show means ± SEM. *, $P < 0.05$; **, $P < 0.01$; ***, $P < 0.001$.

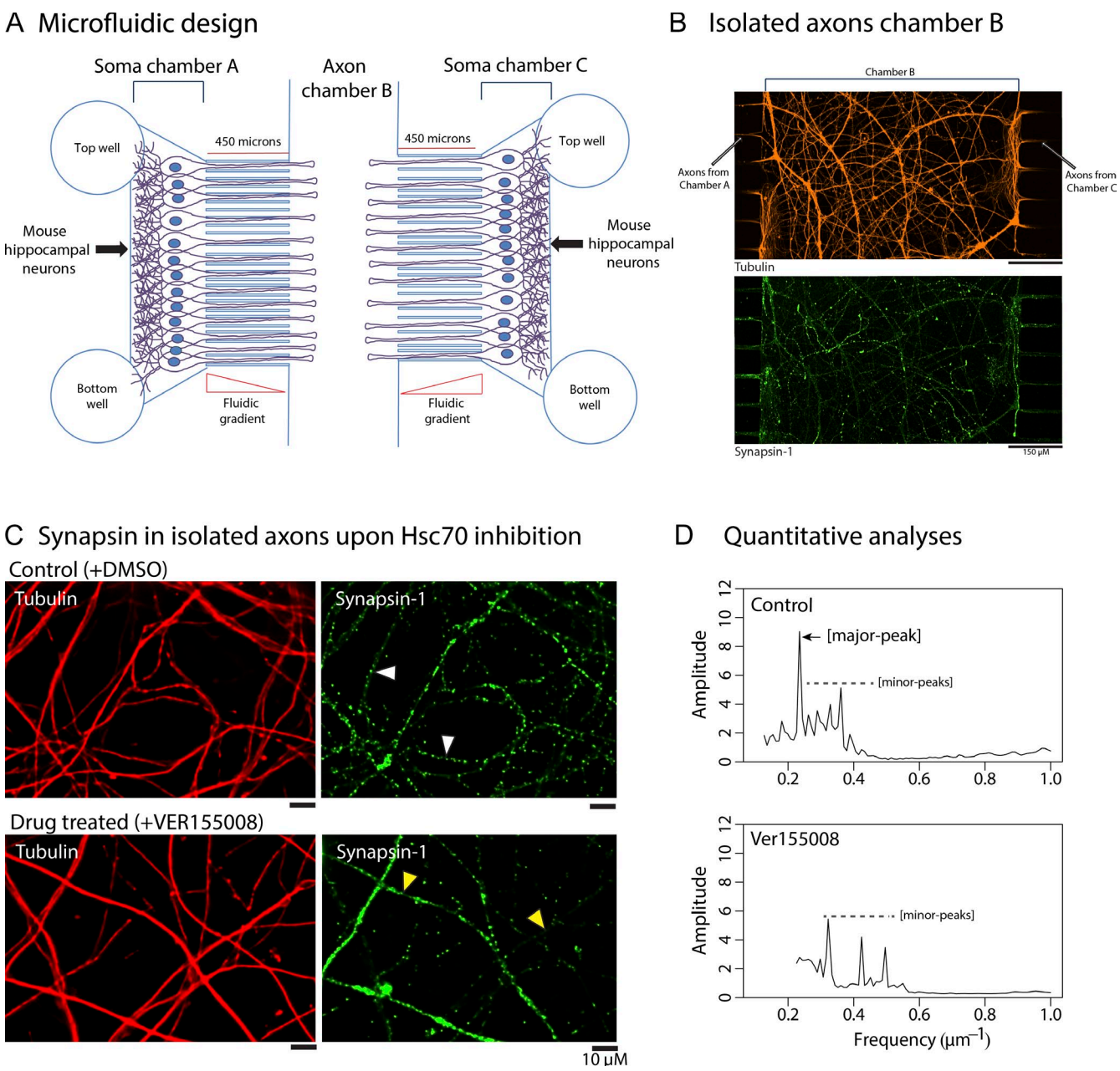

Figure S4. **Disruption of axonal synapsin upon Hsc70 inhibition in isolated axons.** (A) Isolation of axons in the middle chamber of a triple-chambered microfluidic device. Hippocampal neurons are plated in outer chambers (marked A and C), and emanating axons emerge into the central chamber (marked B). Effects of drug treatment on isolated axons were examined by adding drugs only into the axonal chamber. (B) Representative images from chamber B of one such device described in A. The device is fixed at DIV 10 and immunostained for tubulin (to mark axons in chamber B) and synapsin (green). Tubulin staining indicates a dense meshwork of axons from chambers A and C crisscrossing in chamber B (top). (C) Disruption of endogenous synapsin distribution in isolated axons grown in triple-chambered microfluidic devices. Note disruption in the periodic and punctate synapsin distribution upon adding VER155008 to the middle chamber (compare the two axons in top and bottom panels marked with white and yellow arrowheads, respectively). (D) Cumulative FFT plots of line scans from isolated axons (similar to the analysis method in Fig. 7 D) show a loss of the major peak representing the periodic distribution of synapsin (top, black arrow) upon treatment with the Hsc70 inhibitor (bottom).

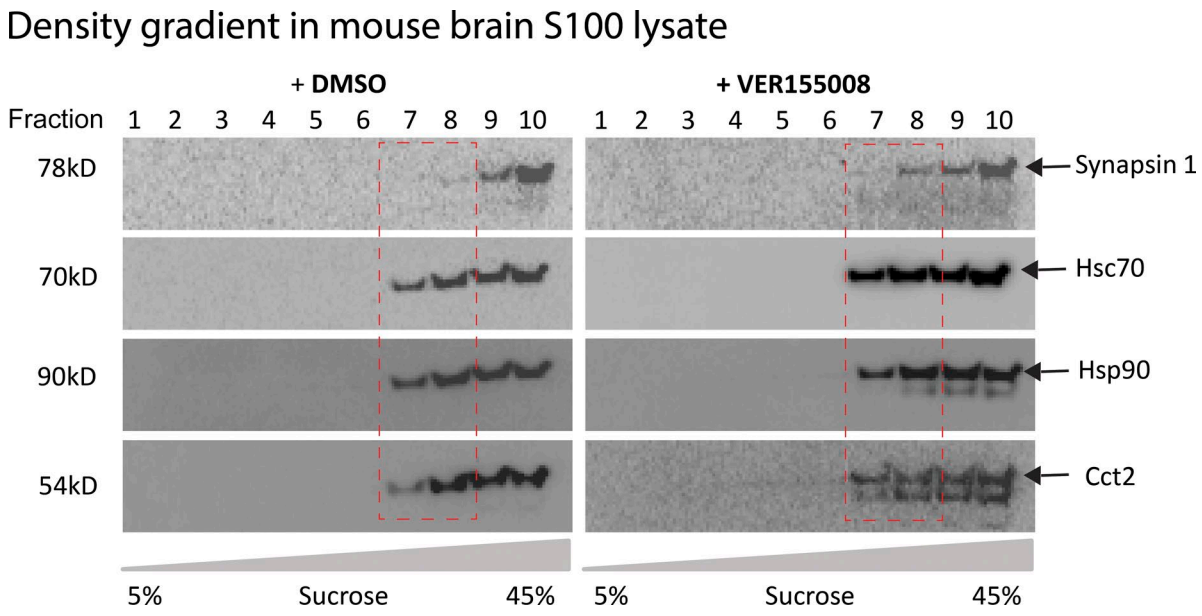

Figure S5. **Density gradients of S100 fractions from mouse brains blotted with synapsin and members of the Hsp family pulled down by our proteomics screen.** HSc70, Hsp90, and Cct2 were observed. Note that all these SCb proteins are localized to high-density fractions like other SCb proteins (Scott et al., 2011; Twelvetrees et al., 2016). Also note subtle changes in distribution of these proteins upon Hsc70 inhibition (fractions within dashed red box).

Table S1 is a separate Excel file showing a list from P2 fractions.
Table S2 is a separate Excel file showing a list from S100 fractions.
Table S3 is a separate Excel file showing a list from P100 fractions.
Table S4 is a separate Excel file showing a list of synapsin interactors from literature found in P100 + S100 fractions.

References

Scott, D.A., U. Das, Y. Tang, and S. Roy. 2011. Mechanistic logic underlying the axonal transport of cytosolic proteins. *Neuron.* 70:441–454. http://dx.doi.org/10.1016/j.neuron.2011.03.022

Twelvetrees, A.E., S. Pernigo, A. Sanger, P. Guedes-Dias, G. Schiavo, R.A. Steiner, M.P. Dodding, and E.L. Holzbaur. 2016. The dynamic localization of cytoplasmic dynein in neurons is driven by kinesin-1. *Neuron.* 90:1000–1015. http://dx.doi.org/10.1016/j.neuron.2016.04.046